

PCCP

Accepted Manuscript



This is an *Accepted Manuscript*, which has been through the Royal Society of Chemistry peer review process and has been accepted for publication.

Accepted Manuscripts are published online shortly after acceptance, before technical editing, formatting and proof reading. Using this free service, authors can make their results available to the community, in citable form, before we publish the edited article. We will replace this *Accepted Manuscript* with the edited and formatted *Advance Article* as soon as it is available.

You can find more information about *Accepted Manuscripts* in the [Information for Authors](#).

Please note that technical editing may introduce minor changes to the text and/or graphics, which may alter content. The journal's standard [Terms & Conditions](#) and the [Ethical guidelines](#) still apply. In no event shall the Royal Society of Chemistry be held responsible for any errors or omissions in this *Accepted Manuscript* or any consequences arising from the use of any information it contains.

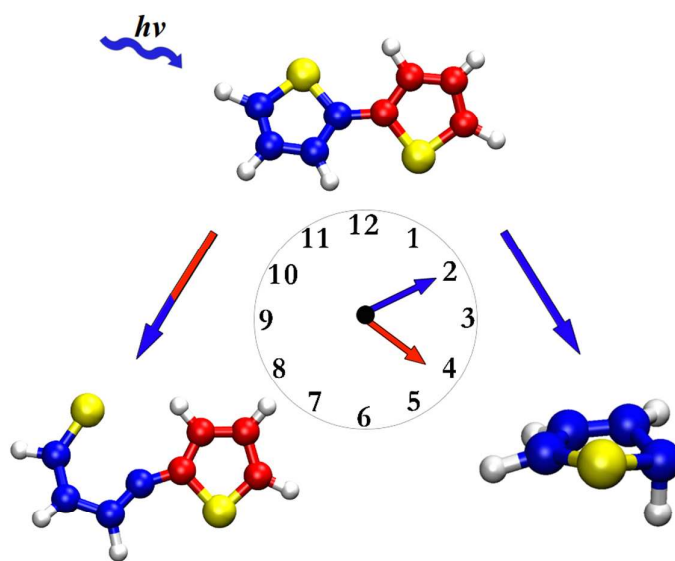
Excited State Dynamics of Thiophene and Bithiophene: New Insights into Theoretically Challenging Systems

Antonio Prlj,[†] Basile F. E. Curchod,^{†,‡} and Clémence Corminboeuf^{*†}*

[†]Institut des Sciences et Ingénierie Chimiques, École Polytechnique Fédérale de Lausanne, CH-

1015 Lausanne, Switzerland

[‡]Department of Chemistry, Stanford University, Stanford, California 94305, United States



Nonadiabatic Dynamics with ADC(2)

Abstract

The computational elucidation and proper description of the ultrafast deactivation mechanisms of simple organic electronic units, such as thiophene and its oligomers, is as challenging as it is contentious. A comprehensive excited state dynamics analysis of these systems utilizing reliable electronic structure approaches is currently lacking, with earlier pictures of the photochemistry of these systems being conceived based upon high-level static computations or lower level dynamic trajectories. Here a detailed surface hopping molecular dynamics of thiophene and bithiophene using the algebraic diagrammatic construction to second order (ADC(2)) method is presented. Our findings illustrate that ring puckering has important role in thiophene photochemistry and that the photostability increases when going upon dimerization into bithiophene.

Keywords: thiophene, bithiophene, surface hopping, ADC(2)

1. Introduction

Owing to its prevalent role in biology and optoelectronics, organic photochemistry^{1,2} has received considerable experimental and theoretical interest. Aided by theory, experimental data can now be interpreted in previously unrealized ways. Concepts such as electronic potential energy surfaces and conical intersections³ enhance understanding of phenomena that occur upon photoexcitation. Special attention has been devoted to the ultrafast deactivation mechanisms of small heteroaromatic molecules including pyrrole,^{4,5} furan,^{6,7} imidazole,⁸ as well as others. On one hand, such simple systems represent fundamental building blocks of many biomolecules in which excited state deactivation may play important biological roles.⁹ On the other hand, thiophene is the most illustrative molecular unit for optoelectronic applications;^{10,11} oligomers and polymers of this species dominate the field of organic electronics being utilized in solar cells,^{12,13} light emitting diodes,^{14,15} photoswitches¹⁶ etc. It is the omnipresence of thiophene that has prompted fundamental research on its electronic properties, particularly on its excited states.

The fact that thiophene is non-fluorescent has been known for some time.¹⁷ Ultrafast radiationless decay was confirmed by Weinkauff et al's pump-probe experiments¹⁸ and interpretations by Marian et al.¹⁹ Their TDDFT (time dependent density functional theory) and DFT-MRCI (density functional theory – multireference configuration interaction) computations, indicated that a ring opening mechanism is responsible for the internal conversion from the excited to the ground state, where deactivation is succeeded by a final ring closure.¹⁹ In line with these results, surface hopping

molecular dynamics simulations by Cui and Fang²⁰ initiated in the first singlet excited state (S_1) and employing the complete active space self-consistent field method (CASSCF) implied that ring opening through C-S bond cleavage is the sole deactivation mechanism from the S_1 state. Alternatively, Stenrup²¹ suggested that the ring puckering mechanism could play a role based on scans of the CASPT2 (complete active space perturbation theory of second order) potential energy surfaces. Deactivation through a ring deformation event is known from pyrrole and furan photochemistry,^{4,7} making it somewhat curious that such a mechanism was not previously identified for thiophene. Most recently, Fazzi and co-workers presented a nonadiabatic molecular dynamics of the excited states of thiophene (and oligothiophenes) using TDDFT.²² Whereas a relaxation process through the ring puckering mechanism was identified, these results are called into question owing to failures found in TDDFT spectra (e.g., spurious state inversion and excitation characters, wrong distribution of oscillator strengths and erroneous potential energy surfaces which are independent from the exchange-correlation functional used in the TDDFT computation).^{23,24}

Since a full reliable theoretical study of the photochemistry of thiophene and its related oligomers appears to be lacking, here, we provide a surface hopping molecular dynamics study of thiophene using the algebraic diagrammatic construction to second order^{25,26} (ADC(2)) method. Our findings verify that the ring puckering process indeed does play a critical role in the deactivation process, even when dynamic simulations are initiated on the S_1 potential energy surface. This mechanism operates

on the same timescale as the ring opening mechanism, making experimental distinction more difficult. As opposed to CASSCF, which has the formal advantage in treating conical intersections, but misses essential dynamic correlation effects, ADC(2) is a correlated single-reference method. The method is sometimes seen as a “MP2 for excited states” and often considered as a compromise to EOM-CCSD in terms of accuracy *vs* efficiency for electronic-state calculations²⁷ (for a detailed discussion on the ADC(2) formalism, the reader is referred to recent reviews^{28,27}). ADC(2) has been successfully applied to an important number of molecular systems²⁸⁻³⁰ and, more specifically, for thiophene-based molecules.^{23,31,32} In the case of thiophene,²³ ADC(2) reproduces the electronic state ordering given by CASPT2 at the ground-state geometry, while TDDFT suffers from its approximation and inverts the character of the first two electronic states. When it comes to excited-state properties and dynamics, ADC(2) is considered to be more robust than CC2 (approximate coupled cluster singles and doubles) as its eigenvalue problem is Hermitian.^{27,33,34} It is for example known that in the region of a conical intersection between excited states of same symmetry, CC2 excitation energies can become complex whereas ADC(2) behaves properly.²⁷ ADC(2) (which formally scales as n^5 with the number of orbitals) is therefore a method of choice for excited-state dynamics^{33,34} and has recently been combined with trajectory surface hopping, providing non-radiative decays for 9H-adenine in good agreement with higher-level methods.³³

In contrast to thiophene, the photochemical processes of bithiophene have been examined only by static computations³⁵⁻⁴⁰ with the exception of the recent TDDFT

study of Fazzi and co-workers.²² In the present study, we find that bithiophene preserves the key features of thiophene photochemistry, including the ring opening mechanism. However, we also find the lowest singlet excited state to have a significantly increased photostability, which may be linked with the wide-ranging application of oligothiophenes in optoelectronic devices. In fact, the increased photostability of the singlet state points to the possibility of intersystem crossing, as suggested by earlier studies.^{17,38}

2. Computational details

The ground state structures of thiophene and bithiophene and corresponding vibrational frequencies were obtained at the MP2/def2-TZVP⁴¹ level. Excited states were consistently computed at the ADC(2)/def2-SVPD⁴² level. Adiabatic excitation energies were computed by optimizing ground and excited state structures with the def2-SVPD basis set. The absorption spectra and the initial conditions for the nonadiabatic dynamics simulations of both systems were computed for geometries and nuclear momenta sampled from an uncorrelated Wigner distribution (0K),^{43,44} as implemented in Newton-X package.⁴⁵ 700 initial conditions (structures and momenta) were sampled for each compound from the Wigner distribution computed from harmonic vibrational frequencies in the ground state. For each structure, vertical excitation energies (the 5 lowest singlet states) and oscillator strengths were computed and the spectral transitions were broadened by Lorentzian with phenomenological broadening of 0.05 eV. The same set of initial conditions was used for the nonadiabatic ab initio dynamic simulations. With the assumption of the initial vertical

excitation, a swarm of trajectories was propagated in the excited states where nuclear motion was treated classically. Nonadiabatic effects were treated by Tully's fewest switches surface hopping method⁴⁶ with the decoherence correction ($\alpha=0.1$).⁴⁷ The microcanonical (NVE) framework was used. In total, 200 trajectories for thiophene with maximal time of 400fs and 100 trajectories for bithiophene with maximal time of 500fs were computed, with a nuclear time step of 0.5fs. Due to methodological difficulties, i.e., the absence of nonadiabatic couplings between the ADC(2) excited states and their underlying MP2 ground state, the hopping to the ground state was not considered and all the trajectories were terminated after reaching the crossing point between the excited (running) state and the ground state.^{33,34} It is furthermore important to note that in Newton-X nonadiabatic couplings are not directly computed from the ADC(2) electronic wavefunction, but rather from a CIS-like reconstructed wavefunction. For more information about the ADC(2) based surface hopping, the reader can refer to ref. 33 and 34.

All ADC(2) and MP2 computations were performed with Turbomole 6.5,⁴⁸ employing the resolution of identity and frozen core approximations. The dynamic simulations were performed with the Newton-X software⁴⁵ interfaced to the Turbomole 6.5 program suite. Molecular structures were visualized with VMD 1.9.1 program.⁴⁹ Finally, due to the unavailability of spin-orbit coupling matrix elements at the ADC(2) level, the former were computed with TDDFT (PBE0⁵⁰/ZORA-DZP⁵¹), using the Zeroth Order Regular Approximation (ZORA) Hamiltonian,⁵² as implemented in Amsterdam Density Functional (ADF2013.01 release) program package.^{53,54,55} EOM-

CCSD calculations for bithiophene were converged with jun-cc-pVTZ basis set⁵⁶ with Gaussian09 program package.⁵⁷

3. Results and discussion

3.1. Vertical Excitation Energies and Spectra

Low-lying excited states of thiophene include two $\pi\pi^*$ states (A_1 and B_2) which account for most of the absorption intensity and a slightly higher antibonding $\pi\sigma^*$ state (B_1) responsible for the ring opening process. Achieving a balanced description of these states using electronic structure methods is not an easy task. In a recent letter²³ we showed that CIS (configuration interaction singles) and TDDFT invert ordering of the two $\pi\pi^*$ states. This is somewhat surprising for TDDFT, which is usually considered reliable for $\pi\pi^*$ states. Nevertheless, standard functionals are unable to provide a picture comparable to reference wavefunction methods due to shortcomings affecting the treatment of both exchange and correlation. On the other hand, $\pi\sigma^*$ states (B_1 and A_2) have a pronounced diffuse character and can also be assigned as $\pi\sigma^* + \text{Rydberg}$ transition. A similar state exists in pyrrole causing the dissociation of the N-H bond,⁴ and its correct assignment was questioned in the literature.⁵⁸ For a good description of such $\pi\sigma^*$ states basis set should contain at least few diffuse functions. In the present work, we use ADC(2) with a def2-SVPD basis set that satisfies this criterion. Although relatively small, this basis set yields results similar to larger basis sets, for a computational cost lower than a triple-zeta basis set. This is especially important in the context of nonadiabatic ab initio dynamics, which

relies upon a good balance between accuracy and computational efficiency. Table 1 compares our vertical excitation energies with the reference results taken from the literature. The excitation energies to the triplet states are listed in the supporting information.

Table 1. Comparison of vertical excitation energies (in eV) and corresponding oscillator strengths (in parentheses) obtained with ADC(2)/def2-SVPD and the values from the literature, as well as EOM-CCSD/jun-cc-pVTZ. Several numbers were not reported or did not converge (-). For details on the molecular geometries and basis sets used see the original articles.

Thiophene	$A_1(\pi_2\pi_4^*)$	$B_2(\pi_3\pi_4^*)$	$B_1(\pi_3\sigma^*)$	$A_2(\pi_2\sigma^*)$	$A_2(\text{Ryd})$
ADC(2)	5.82(0.093)	6.23(0.112)	6.45(0.011)	6.60(0.0)	6.77(0.0)
MS-CASPT2 ²¹	5.85(0.067)	6.14(0.109)	6.57(0.0)	6.65(0.0)	-
EOM-CCSD ⁵⁹	5.78(0.081)	6.13(0.084)	6.33(0.013)	6.37(-)	6.19(-)
DFT-MRCI ¹⁹	5.39(0.114)	5.54(0.112)	5.86(0.004)	6.10(0.0)	5.88(0.0)
Bithiophene	$B(\pi_6\pi_7^*)$	$A(\pi_5\pi_7^*)$	$B(\pi_4\pi_7^*)$	$A(\pi_6\sigma^*)$	$B(\text{Ryd})$
ADC(2)	4.59(0.445)	5.32(0.007)	5.47(0.146)	5.70(0.002)	5.80(0.002)
EOM-CCSD	4.62(0.378)	5.38(0.006)	5.50(0.097)	5.67 (0.008)	-
SS-CASPT2 ³⁹	4.11(0.32)	-	5.14(0.13)	-	-

To gain a better insight into the character of the excited states listed in Table 1, the most relevant molecular orbitals are displayed in Figure 1. It is well known that the Hartree-Fock orbitals may significantly change their shape depending on the size of

the basis set,⁶⁰ while the excitations can be expressed with a large number of orbital transitions having sizeable amplitudes. For that reason, we find more convenient to display transition natural orbitals, which better reflect the main character of the states. The natural transition orbitals are used here only in a qualitative way, but we notice that they were computed by neglecting correlation effects in the ground state and the double excitations in excited states.

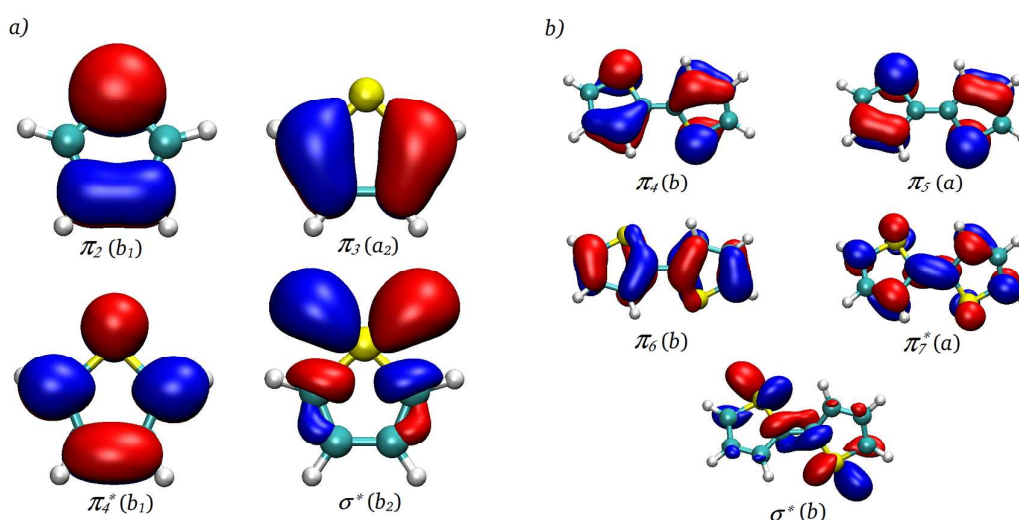


Figure 1. (Natural transition) orbitals involved in the lowest singlet transitions of a) thiophene and b) bithiophene (isovalue=0.04).

For thiophene, a reasonable agreement is achieved between our ADC(2) vertical excitation energies, the CASPT2 results of Stenrup²¹ and the EOM-CCSD (equation of motion – coupled cluster singles doubles) of Holland et al.⁵⁹ The Rydberg state (A_2) is higher in energy with ADC(2), although this should have no effect on the dynamics in the low-lying states. The DFT-MRCI energies computed by Marian et al.¹⁹ are somewhat lower and closer to the experimental peak maxima measured at

5.26⁶¹/5.48⁶² eV for $A_1(\pi\pi^*)$ and 5.64⁶¹/5.93⁶² eV for $B_2(\pi\pi^*)$ state. However, it is known that vertical excitation energies should not be strictly compared to the experimental band maxima^{63,64} and this is especially true for thiophene, which is characterized by a strong coupling between the two $\pi\pi^*$ states.^{19,21} Instead, a more suited comparison is achieved with the adiabatic ($\Delta E_{0,0}$) excitation energies. In this respect, our $\Delta E_{0,0}$ energy for the A_1 minimum (5.17 eV) agrees well with experiment⁶⁵ (5.16 eV), and so does the CASPT2 result of Stenrup²¹ (5.12 eV), and the TDDFT+DFT-MRCI value of Marian et al.¹⁹ (5.16 eV) (zero point energy corrections are not taken into account in all three cases). Whereas our recent study demonstrated that TDDFT yields incorrect geometries,²³ this issue was resolved by Marian et al.¹⁹ through imposing a symmetry constraint. The elusive $B_2(\pi\pi^*)$ minimum is a more intriguing question. For this state, the $\Delta E_{0,0}$ was never determined experimentally⁵⁹ and no minimum was found at the CASPT2 level,²¹ implying that the B_2 state is most likely unbound. Our ADC(2) computations support this view as no B_2 minimum was located. The geometries resulting from TDDFT²³ and CASSCF⁶⁶ optimizations are most likely spurious.

The vertical excitation energies of bithiophene are also reported in Table 1. Good agreement was found between ADC(2) and EOM-CCSD results computed on the same geometry. The CASPT2 energies of Andrzejak and Witek³⁹ are lower than our ADC(2) values. However, they correspond to the C_{2h} symmetric structure whereas the true ground state minimum is not planar.⁶⁷ Imposing planarity lowers the ADC(2) excitation energies to 4.34 and 5.45 eV for the two bright $\pi\pi^*(B)$ states. It is not

surprising that the excitation energy of S_1 decreases significantly upon planarization: the excited state gets stabilized (S_1 has a planar minimum²³) and the ground state destabilized. When converging our results further using a large basis set (aug-cc-pVTZ⁶⁸), the energies of 4.22 and 5.36 eV compare well with the CASPT2 values. Differences of 0.1-0.2 eV are within the accuracy of ADC(2), which has mean error of 0.22 eV.²⁸ The S_3 state (as well as S_2) is rather sensitive to the perturbative double excitations as shown by the CIS/CIS(D) diagnostics.²³ Given that ADC(2) treats the double excitations only approximately, the energy of the two states may be slightly overestimated. On the other hand, the CASPT2 excitation energies of the two bright $\pi\pi^*$ states are anticipated to be highly sensitive to the active spaces, basis sets etc.^{35,37,39} Andrzejak and Witek³⁹ demonstrated that earlier CASPT2 computations^{35,37} were erroneously predicting the two states as quasi-degenerate, whereas the actual gap is as large as 1 eV when using large basis sets and a variety of active spaces.

Finally, we show the absorption cross sections for both thiophene and bithiophene computed with the semiclassical Wigner distribution approach at the ADC(2)/def2-SVPD level. The simulated spectra confirm that the band maxima are slightly red-shifted with respect to the vertical excitation energies. The spectra were decomposed into contributions from different states, S_1 (blue) and S_2 (red) for thiophene, S_1 (red) and S_3+S_4 (blue) for bithiophene. The color code is consistent with the one used in our previous study,²³ and reflects the character of the $\pi\pi^*$ states. The energy windows used for the sampling of the initial conditions of molecular dynamics simulations are also indicated.

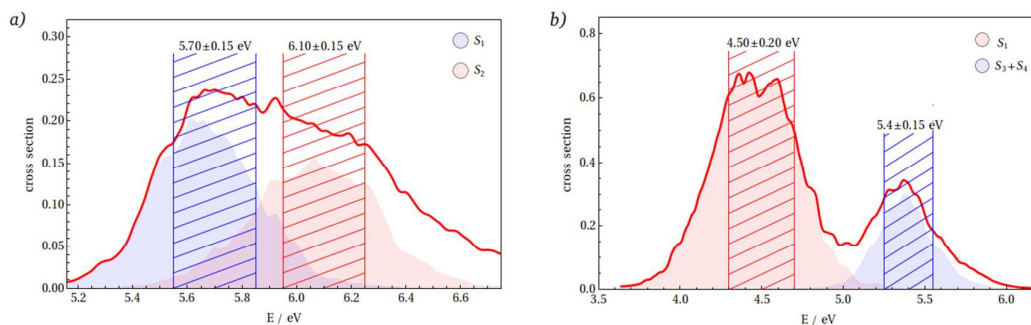


Figure 2. Photoabsorption spectra computed from Wigner distribution of: a) thiophene and b) bithiophene at ADC(2)/def2-SVPD level.

3.2 Excited State Dynamics of Thiophene

In contrast to the earlier CASSCF surface hopping study,²⁰ which was applied only from the first excited state, the present dynamics is initiated from both S_1 and S_2 , which have comparable intensities (Figure 2a). Initial conditions were chosen randomly from the narrow energy windows approximately centered at the vertical excitation energies. A swarm of 100 trajectories was initiated from both states and nonadiabatic couplings were computed for the first four excited states. Since no couplings were computed between the ground (MP2) and excited (ADC(2)) states, the dynamics was terminated at their crossing point. The sole consideration of the excited state dynamics suffices to identify the major deactivation paths. The main underlying assumption is that in the crossing region electronic population is transferred to the ground state while recurrences represent only a minor effect. Similar protocols were also adopted in earlier ADC(2)^{33,34} and TDDFT^{4,8} surface hopping studies.

Two internal conversion mechanisms characterize the thiophene photochemistry: the ring opening due to the CS bond cleavage and the ring puckering arising from the out-of-plane distortions. The ring opening is favored and accounts for 83% and 70% of the deactivation pathways from S_1 and S_2 respectively, while the rest of the trajectories proceed via ring puckering. The energy profiles of four illustrative trajectories are shown in Figure 3, although alternative scenarios are possible. In Figure 3a, the molecule is initially excited in the S_1 state having a dominant $\pi_2\pi_4^*$ character. The trajectory evolves on the S_1 potential energy surface, which eventually changes into $\pi_3\pi_4^*$ and $\pi_3\sigma^*$ character. This is followed by the elongation of the CS bond distance and an increase of the ground state energy, which after an approximate total time of 80fs crosses the first excited state. More detailed analysis of this trajectory (as well as the one shown in Figure 3c) can be found in SI. The second trajectory (Figure 3b) was initiated in the S_2 state with a dominant $\pi_3\pi_4^*$ character. Surface hopping to $S_1(\pi_2\pi_4^*)$ occurs around 15fs leading finally to the ring opening owing to the antibonding $\pi_3\sigma^*$ nature of the S_1 potential energy surface. Note that the major dynamical changes occur both nonadiabatically (i.e., surface hopping due to the strong nonadiabatic coupling) and adiabatically (i.e., within the same adiabatic state) by a change in electronic character. The latter suggests that the corresponding diabatic states are strongly coupled through nondiagonal matrix elements of the electronic Hamiltonian. Note however that in the present context the concept of diabatic states is used in a rather non-mathematical way to assign the main orbital configurations of the excited states. Akin to the first trajectory, Figure 3c shows a system evolving

adiabatically on the S_1 potential energy surface. Initial $\pi_2\pi_4^*$ character changes into $\pi_3\pi_4^*$ leading to the ring puckered intersection with the ground state. The final structure is characterized by a deplanarized ring and a sp^3 hybridization of the carbon atom adjacent to sulfur. The last example features several hops but the running state preserves the main $\pi_3\pi_4^*$ character. The trajectory ends with the ring puckering after a total time of roughly 100fs. Since the ring puckering occurs at the crossing between the $\pi_3\pi_4^*$ state (B_2 irrep in C_{2v} point group) and the ground state, it is not surprising that its probability increases for the trajectories initiated in the S_2 state. However, the higher energy window, which is closer to the antibonding $\pi\sigma^*$ state, also facilitates ring opening. Overall, the deactivation is not strongly dependent on the initial excitation energies although puckering becomes more important at higher energies. The ultrafast decay was accomplished by all 200 computed trajectories within a time significantly shorter than the maximal time set to 400fs.

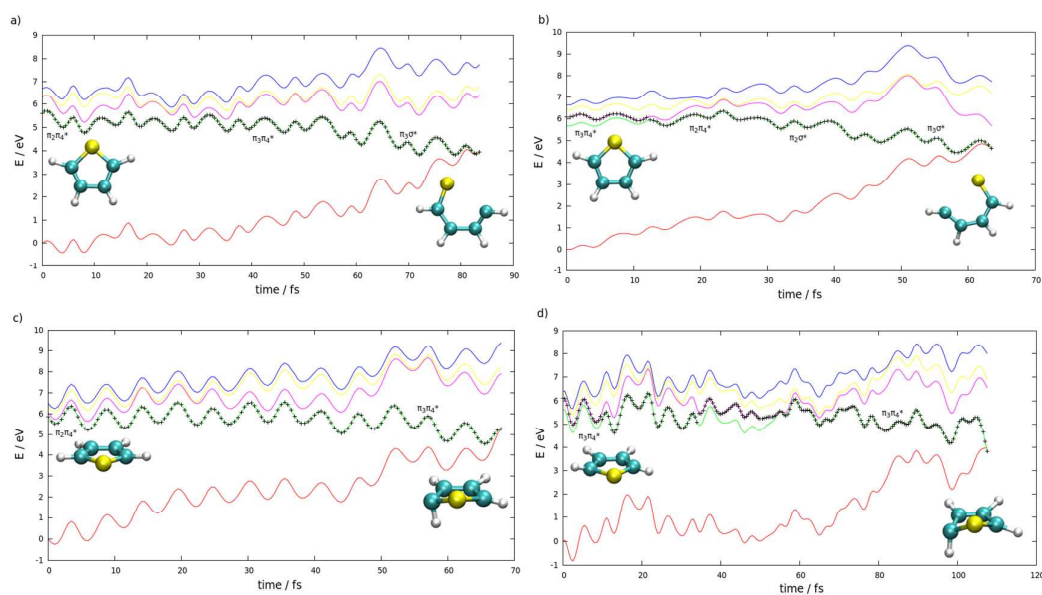


Figure 3. Energy profiles of the four trajectories following a,b) ring opening and c,d) ring puckering mechanism. Trajectories were initiated on a,c) S_1 and b,d) S_2 potential energy surface. The time evolution of the ground and four lowest excited adiabatic singlet states are displayed in color, whereas the running state is indicated in black. The energies are plotted relative to the initial ground state energy (0fs). Molecular geometries at the initial and final step of the dynamics are given for each trajectory. The Figures on the left are “adiabatic” while those on the right are nonadiabatic, i.e., with surface hops.

Although specific trajectories may indicate possible relaxation paths that molecules can undergo, in surface hopping properties should be monitored over the full swarm of trajectories, which is expected to mimic the dynamics of a nuclear wavepacket (within a semiclassical approximation⁶⁹). In Figure 4 we show a time evolution of the average CS bond lengths (as both CS bonds in thiophene can break) for trajectories initiated in each of the two states (S_1 and S_2). The final steps representing the crossing between the first excited and the ground states are given in black. In both cases, the initial elongation of the CS bond occurs already in the $\pi\pi^*$ states owing to their nature. This motion efficiently couples with the higher $\pi\sigma^*$ state, resulting in the ultrafast decay of most of the trajectories before 100fs. The rest of the trajectories persists up several hundred femtoseconds. This observation is consistent with the earlier CASSCF dynamics²⁰ where a time constant of 65 ± 5 fs was obtained for 80% of the trajectories. However, a non-negligible portion of the trajectories terminates with the

ring puckering, which is represented by the black dots in the lower part of the graphs.

The timescales on which the two mechanisms operate are indistinguishable.

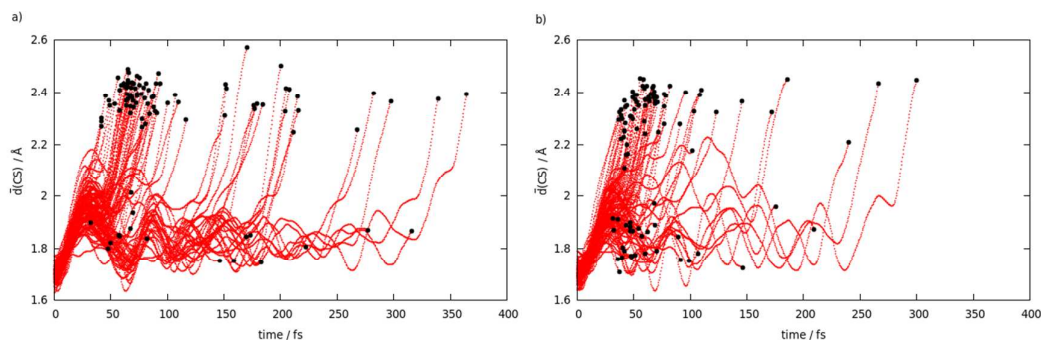


Figure 4. Time evolution of the average CS bond lengths for trajectories initiated on the a) S_1 and b) S_2 potential energy surface. The steps of the nonadiabatic dynamics are represented by the red dots while the final points are marked in black.

The out-of-plane motions of the hydrogen atoms next to sulfur (i.e., the δ_{CCH} dihedral angle) can also distinguish the puckering from the ring opening and is chosen as another collective variable (the average value was considered for both H atoms).

Figure 5 demonstrates how do the swarms split into two regions, representing two internal conversion mechanisms. The geometrical parameters of the CASPT2²¹ optimized S_1/S_0 conical intersections and S_1 minimum are also plotted for comparison. The scattering of dots representing crossing points from the simulations is mainly due to the dynamical effects. As noted by Tully,⁷⁰ the actual probability that an arbitrary trajectory will pass exactly through a conical intersection is equal to zero. The proximity of a conical intersection is more relevant as it represents the region of small energy splitting and large nonadiabatic couplings, resulting in a high probability of nonadiabatic transition. The intersection region seems to be qualitatively well

described by ADC(2). However, the ring opening appears at somewhat lower CS distances ($\sim 3\text{\AA}$) as compared to the optimized CASPT2 conical intersection (3.4\AA ; in Figure 3 only the average value is shown). Stenrup²¹ also reports a shallow minimum very close to the ring opened conical intersection, which we do not find at the ADC(2) level. Such discrepancies could be expected given that ADC(2) is not very accurate for distorted geometries close to the conical intersections with the ground state. The method lacks double excitations and is based on the MP2 single reference ground state. The latter aspect is illustrated by the rapid increase of the D1 diagnostic as the trajectory approaches the crossing with the ground state (see SI). The analysis of the D1 parameters also shows that in the course of the simulations, the molecule indeed spends most of the time in the region where the method is reliable. Out-of-plane distortions also play important role in the excited state dynamics of thiophene as indicated by the region with a high density of red points, which coincides with the nonplanar S_1 minimum. Such motions also prompt ultrafast deactivation via ring puckering. Stenrup²¹ distinguishes two types of puckering, one mainly on the sulfur atom (CI b) and another on the carbon atom (CI c). The analysis of our geometries reveals that only several crossing points are associated with the conical intersection of the c type, while most of the structures resemble to the conical intersection of type b (see insets in Figure 3). Furthermore, we find another type of puckering where distortion occurs on C atom opposite to S, although the corresponding trajectory was not part of the original set of calculations (see SI).

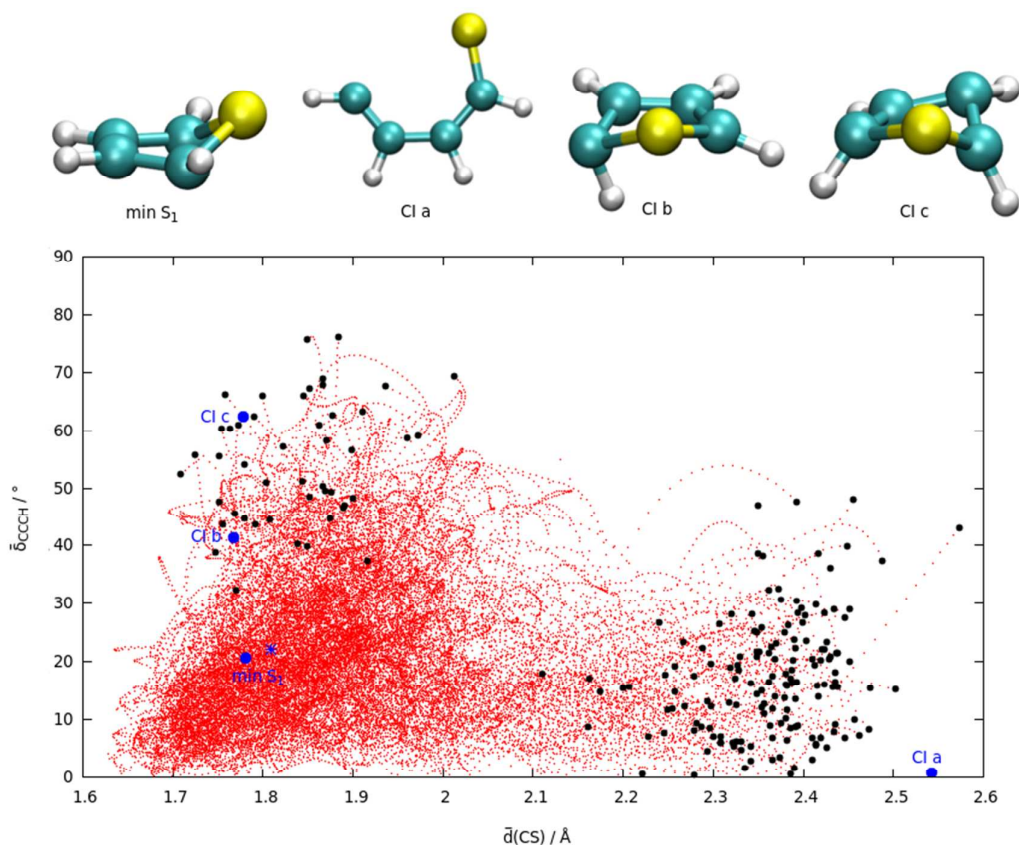


Figure 5. Evolution of the average bond length distances and CCCH dihedral angles of all 200 thiophene trajectories. The steps of the dynamics are represented in red, while the final crossing steps are marked in black. The dihedral angle was redefined in the range between 0° and 90°. The structures associated with the CASPT2-optimized conical intersections and S₁ minimum were taken from the supporting information of reference 21 and are represented in blue. For comparison, the S₁ minimum obtained at the ADC(2)/def2-SVPD level is shown as a blue asterisk.

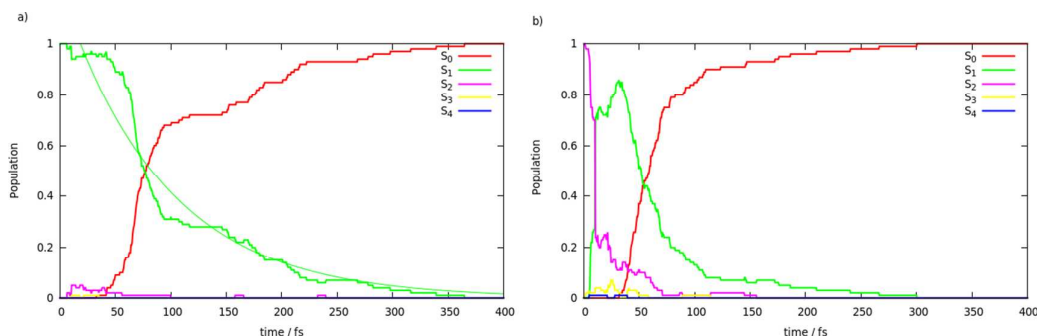


Figure 6. Time evolution of the average populations of the ground and first four singlet excited states for the trajectories started in a) S₁ and b) S₂ state.

The average populations of the individual excited states shown in Figure 6, mirror the timescales on which the internal conversion processes occur. As noted earlier, it is assumed that the molecule will relax in the ground state after the crossing. For the first set of trajectories initiated in S₁ (Figure 6a), the decay seems more complex than an exponential but the appearance of a small knee at around 100fs, might be due to a sampling issue. The overall decay time is nevertheless calculated from the population fitted to a single exponential function $f(t)=\exp[-(t-t_d)/t_e]$ where t_d is a latency time and t_e the exponential time constant. For the S₁ dynamics $t_d=18$ fs and $t_e=93$ fs so that total time constant (t_d+t_e) is equal to 111fs. Based on both pump-probe photoelectron spectroscopy and theoretical modeling, the lifetime provided by Weinkauff et al.¹⁸ is expected to be in the 100fs regime, which is in line with our results. Note, however, that direct comparison is restricted since the experiment corresponds to an excitation to the lowest S₁ vibrational level. The trajectories initiated on the second excited state (Figure 6b) are characterized by a rapid depopulation of S₂ state occurring in 10fs. Fitting of the assumed S₀ population to an exponential function leads to $t_d=16$ fs and

$t_e=57$ fs. The shorter total time constant is in line with the unbound nature of the B_2 $\pi\pi^*$ state and the larger internal energy associated with the higher energy window.

Overall, our dynamic picture complements the “static” computations of Marian et al.¹⁹ and Stenrup.²¹ An obvious advantage of ab initio nonadiabatic dynamics is the unbiased exploration of the potential energy surfaces, the treatment of nonadiabatic effects and the insight into the timescales. The existence of the ring puckering mechanism is in major disagreement with the CASSCF surface hopping study of Cui and Fang,²⁰ and the TDDFT dynamics of Fazzi et al.²² also predicted both mechanisms. At this point, it is hard to say why CASSCF differs, especially since the authors did not provide the corresponding excitation energies. However, results from the literature show that CASSCF can give various values, depending on the active space, basis set and other parameters. For instance, A_1 and B_2 states ($\pi\pi^*$) were found to be nearly degenerate in Ref 66, whereas in work of Roos et al.⁷¹ B_2 state is placed 1.7 eV above A_1 . Alternatively, Stenrup²¹ notices that CASSCF does not provide a balanced description of the two $\pi\pi^*$ states and the perturbational correction is necessary.

3.3 Excited State Dynamics of Bithiophene

Despite the considerable interest in small oligothiophenes, the excited state dynamics of bithiophene was only studied experimentally,^{72,73} with the exception of TDDFT simulations mentioned previously.²² The lowest excited singlet state of bithiophene was shown to decay in a relatively long time (lifetime 51ps)⁷³ and the population

transfer was attributed to an intersystem crossing (ISC) with an ISC rate of 0.99.^{73,17} Note that the experiments^{17,73} were performed in dioxane and benzene. While several quantum chemical studies dealt with singlet and triplet excited states of bithiophene,^{17,36,37,74-76} the most recent one of Weinkauff et. al.³⁸ (including oligothiophenes of chain lengths 2 to 6) attributes efficient intersystem crossing to transition from S_1 state to the lower triplet state T_2 , which subsequently transfers its population to T_1 state. We here compute the excited state dynamics of bithiophene by means of surface hopping trajectories. Our primary focus is the intrinsic (gas phase) dynamical properties of the singlet excited states, while the interplay with the triplets is only considered through single point computations. The full surface hopping dynamics including both singlet and triplet states, and the possibility of the singlet-triplet transitions will be considered in future studies. One of the goals is to establish the similarity between the dynamics of thiophene to its simplest oligomer. As noted before, two bright $\pi\pi^*$ (B) states dominate the low-energy photoabsorption spectrum of bithiophene, giving rise to two distinct peaks. Our simulations were initiated in both $\pi\pi^*$ states. The initial conditions for the surface hopping dynamics from S_1 were sampled from the lower energy window shown in Figure 2b. In contrast to thiophene, which experiences very fast deactivation, bithiophene S_1 dynamics is substantially more stable. Out of 50 trajectories computed with a total time of 500fs and with nonadiabatic couplings between the first four excited states, 71% of the trajectories were stable, while the rest underwent a ring opening (see Figure 7a). We observed no equivalent of the ring puckering mechanism. In the illustrative trajectory (Figure 7a)

leading to the ring opening mechanism system remains in the same state for about 400fs. A surface hopping to the antibonding $\pi\sigma^*$ state occurs after around 420fs, followed by a crossing with the ground state. The transition to the $\pi\sigma^*$ state is alternatively realized by an adiabatic change of character. The CS bond cleavage is therefore due to the lowering of the $\pi\sigma^*$ state from the higher energy manifold.

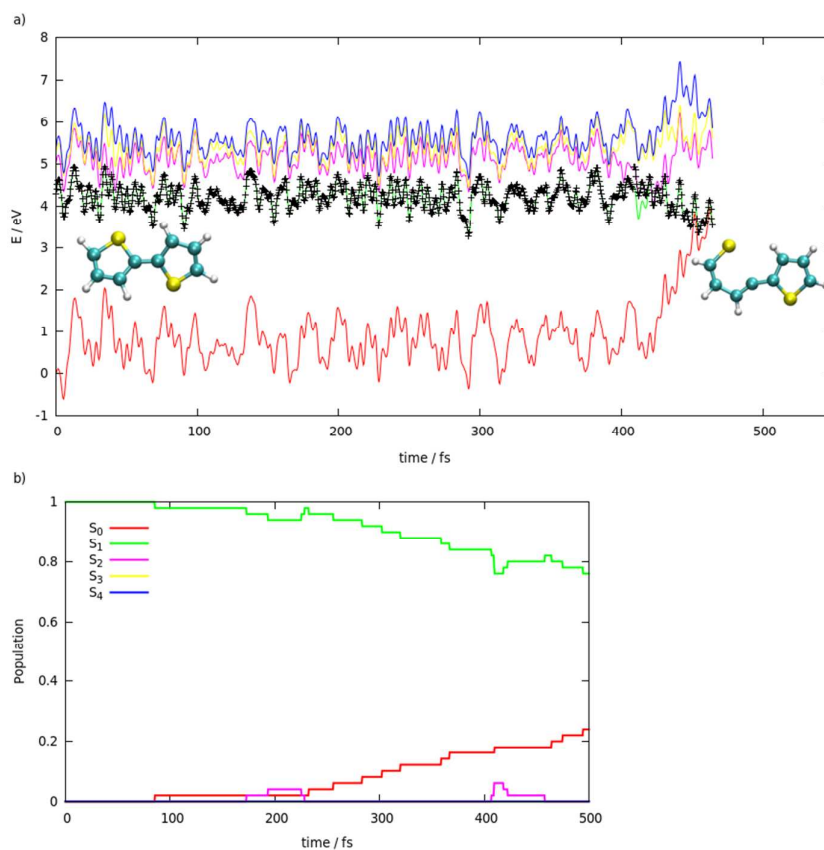


Figure 7. a) A representative ring opening trajectory showing the time evolution of the ground and four lowest excited adiabatic singlet states. The running state is indicated in black. The energies are plotted with respect to the initial ground state energy (0fs). The molecular geometries at the initial and final step of the dynamics are shown. b) The time evolution of the average populations of the ground and first four singlet

excited states for the surface hopping dynamics of bithiophene initiated on the S_1 potential energy surface.

Figure 7b shows that the dynamics is dominated by the S_1 state, while the small population of S_2 is mainly due to the hops to S_2 in the ring opening type trajectories. Although our dynamics study is based on a relatively small number of trajectories and short simulation times, the rough estimate of the S_1 lifetime is 1.8ps with a latency time of 0.1ps. This is certainly not in a good quantitative agreement with the experimental lifetime (51ps).⁷³ At this stage, we cannot exclude that the ring opening is an artifact of our computations or that the solvent inhibits this process. TDDFT simulations²² similarly predict that small fraction of trajectories relaxes by CS bond cleavage. Nevertheless, the crucial finding is that bithiophene evolving in S_1 is much more stable, which opens the possibility for an efficient ISC. The relative stability with respect to the internal conversion mechanisms may be attributed to the energy lowering of the S_1 $\pi\pi^*$ state (being even more pronounced for larger oligothiophene chains) implying that the respective dynamics is less affected by the higher manifold of states. Non-polar organic solvents typically stabilize S_1 for 0.2-0.4 eV.³⁸ In general, the absence of internal conversion is fundamental for any real-life optoelectronic applications, since conversion of (absorbed) energy into geometrical rearrangements such as bond breaking would be detrimental to the device.

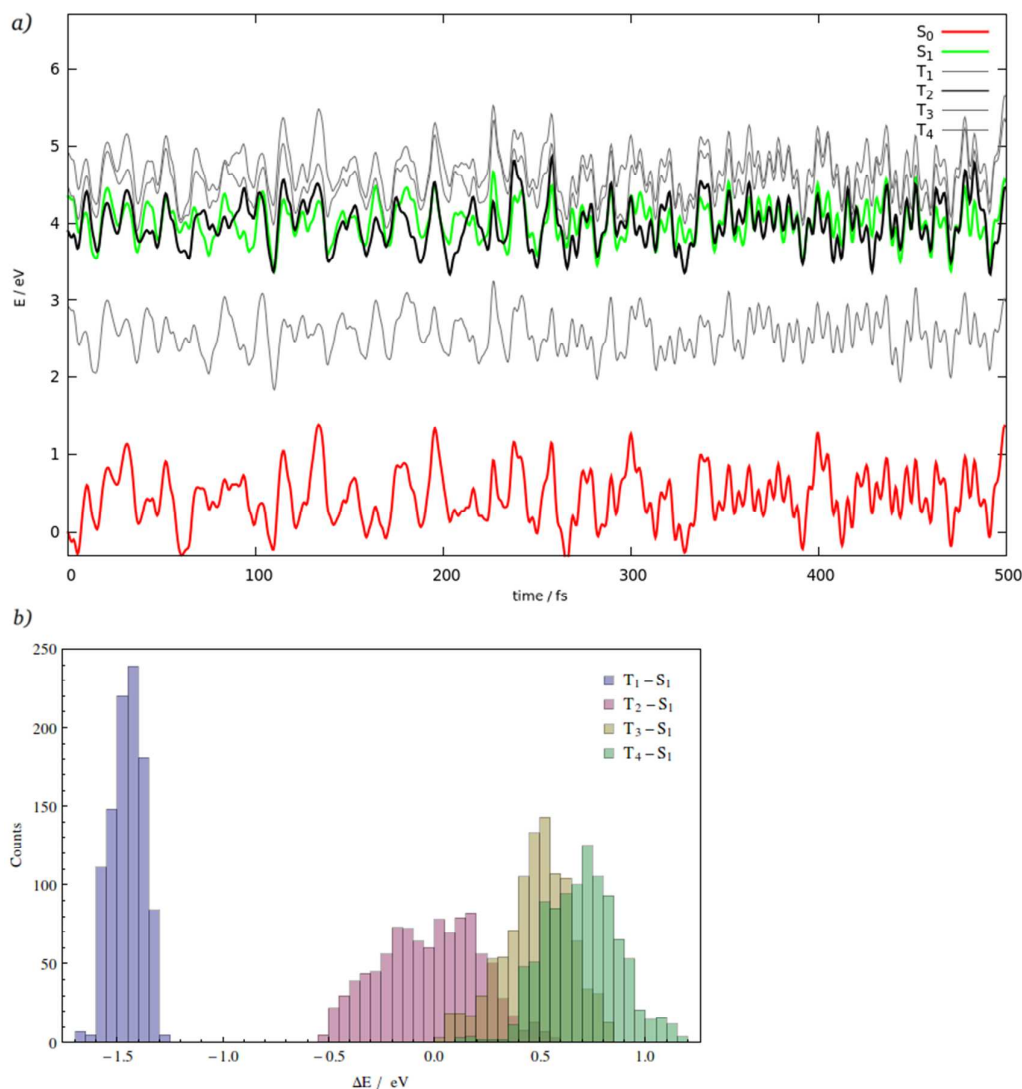


Figure 8. a) Variation of the electronic energies of the four lowest triplet states of bithiophene (T₁, T₃, T₄ gray, T₂ black) for a representative trajectory evolving on the S₁ (green) potential energy surface. The energies are plotted with respect to the initial ground state (red) energy. b) Histogram of the energy gaps between the four triplets and S₁ state based on thousand steps taken from the trajectory in a).

The energies of four lowest triplet states vary through the dynamics on the S₁ (green) potential energy surface (Figure 8a). Evidently, the trajectory running in S₁ experiences multiple crossings with the T₂ state (black). The role of the higher triplet

states is smaller but should not be disregarded. The distribution of T_x-S_1 ($x=1-4$) energy gaps between the four triplets and S_1 state (Figure 8b) shows that T_2 has the largest overlap with S_1 . As S_1 has a planar minimum, group theory restricts the spin-orbit coupling matrix elements between S_1 and T_2 to be zero for the minimum geometry. Therefore, the out-of-plane motions could prompt singlet-triplet transitions, as noted before.³⁸ Such motions are highly active during the S_1 dynamics. The minimum ground state geometry exhibits large inter-ring dihedral angle (experimental 148° ,⁷⁷ in this work 150°) and is slightly bent (molecule does not possess center of inversion). After vertical excitation to S_1 , which is characterized by a planar C_{2h} minimum, the out-of-plane oscillatory motions become significant. Nevertheless, the truthful interpretation of the experimental observation would require additional excited state dynamic studies including spin-orbit couplings and environment effects. In the case of thiophene, the possibility of ISC was invoked by Marian et al.,¹⁹ although it was considered less probable due to the ultrafast internal conversion paths and modest spin-orbit couplings.⁷⁸ On the other hand, weak phosphorescence was experimentally detected⁷⁹ (though not in another study¹⁸) and that question is certainly awaiting additional theoretical investigation. The development of surface hopping with states of different multiplicities is still at its infancy,⁸⁰ but alternative schemes such as SHARC (surface hopping with arbitrary couplings) of Gonzalez et al.⁸¹ and generalized trajectory surface hopping of Cui and Thiel⁸² exist. One discouraging feature is that multireference methods might be overly expensive (and even challenging³⁹) for bithiophene, and even more for larger oligomers. Computationally

cheaper correlated single reference methods such as ADC(2) represent an appealing alternative assuming that spin-orbit couplings will become available in standard quantum chemical codes. Here we only analyze several crossing points (S_1 - T_2) for the trajectory shown in Figure 8a. Based on the approximate TDDFT method we computed spin-orbit coupling matrix elements in the range from 3 to 45cm^{-1} , the latter values being sufficient for effective ISC over the long time.

The final dynamic trajectories were initiated at the higher $\pi\pi^*$ states (with the initial conditions randomly sampled from the window indicated in Figure 2). To ensure that the dynamics starts at the bright state, only the states with large oscillator strengths ($f > 0.05$) were accepted as a proper initial condition. By applying this criterion, a total of 50 trajectories were initiated in S_2 (1), S_3 (36), S_4 (12) and S_5 (1), with the number of respective trajectories indicated in parenthesis. The trajectories were propagated for 500fs and nonadiabatic couplings were computed between first six excited states. As expected, the proximity of the $\pi\sigma^*$ state, results, for most of the trajectories (82%), in a relaxation to the ground state via ring opening. The rest populates S_1 state and remains stable in the course of the dynamics. No analogue of ring puckering was found as for the lower energy window. It is also worth mentioning that the ring opening was observed almost exclusively (for both windows) for the breaking of the “inner” CS bond (next to the CC linker). This is consistent with the localization of the σ^* orbital depicted in Figure 1b. Only a single trajectory initiated from the higher energy window experienced the dissociation through the “outer” CS bond, forming the less stable primary carbon radical. The fitting of the assumed ground state

population increase (Figure 9) through an exponential function leads to an effective time constant of 270fs, corresponding to an ultrafast deactivation process. Two trajectories were discarded from the analysis as they ended with a direct crossing between S_2 and the reference state (S_0), with S_1 being below the reference state (ADC(2) is not reliable in the regions crossing the ground state).

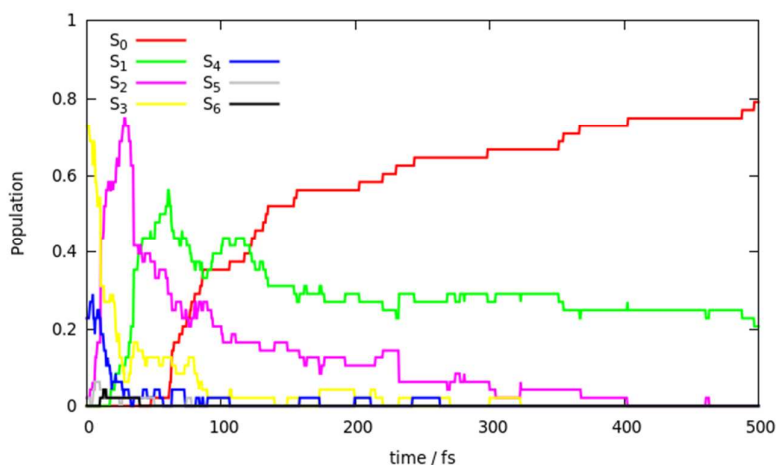


Figure 9. Time evolution of the average populations of the ground and first six singlet excited states of bithiophene for trajectories started at the higher energy window (see Figure 2).

4. Conclusion

The accurate theoretical description of the photochemical processes of thiophene-based molecules may promote our ability to address the most relevant questions associated with applications in the field of organic electronics. We presented a detailed and comprehensive surface hopping molecular dynamics study of thiophene and bithiophene using the algebraic diagrammatic construction to second order method. Our results stress that the ring puckering mechanism plays a critical role in

the deactivation process from the S_1 potential energy surface of thiophene. This mechanism operates on the same timescale as the more representative and previously identified ring opening process. In contrast, the ring opening was the only deactivation mechanism identified from the excited state dynamic trajectories of bithiophene. Furthermore, the lowest excited state of bithiophene was found to exhibit an enhanced photostability illustrated by a much longer lifetime. Our computations also illustrate that correlated single reference methods such as ADC(2) represent an appealing alternative to expensive quantum chemical methods as CASPT2, and has the potential to replace the often used, but more approximate, TDDFT, at least for the small and middle-sized molecular systems.

Acknowledgements Funding from the *European Research Council* (ERC Grants 306528, “COMPOREL”) and the Swiss National Science Foundation (no. 156001).

Supporting Information Available: Details on triplet excitation energies, trajectory analysis and assessment of ADC(2) method. This material is available free of charge via the Internet at <http://pubs.acs.org>.

References

- (1) J. Michl and V. Bonačić-Koutecký, *Electronic Aspects of Organic Photochemistry*, Wiley-Interscience, 1990.
- (2) M. Klessinger and J. Michl, *Excited States and Photochemistry of Organic Molecules*, Wiley-VCH, 1995.
- (3) W. Domcke, D. R. Yarkony and H. Koppel, *Conical Intersections: Theory, Computation and Experiment*, World Scientific Publishing Company, 2011.

- (4) M. Barbatti, J. Pittner, M. Pederzoli, U. Werner, R. Mitrić, V. Bonačić-Koutecký and H. Lischka, *Chem. Phys.*, 2010, **375**, 26.
- (5) D. V. Makhov, K. Saita, T. J. Martinez and D. V. Shalashilin, *Phys. Chem. Chem. Phys.*, 2015, **17**, 3316.
- (6) T. Fuji, J. Suzuki, T. Horio, T. Suzuki, R. Mitić, U. Werner and V. Bonačić-Koutecký, *J. Chem. Phys.*, 2010, **133**, 234303.
- (7) M. Stenrup, Å. Larson, *Chem. Phys.*, 2011, **379**, 6.
- (8) R. Crespo-Otero, M. Barbatti, H. Yu, N. L. Evans and S. Ullrich, *ChemPhysChem*, 2011, **12**, 3365.
- (9) C. E. Crespo-Hernández, B. Cohen, P. M. Hare and B. Kohler, *Chem. Rev.*, 2004, **104**, 1977.
- (10) I. F. Perepichka and D. F. Perepichka, *Handbook of Thiophene-based Materials: Applications in Organic Electronics and Photonics*, John Wiley & Sons Ltd: Chichester, U. K., 2009.
- (11) A. Mishra, C. Ma and P. Bäuerle, *Chem. Rev.*, 2009, **109**, 1141.
- (12) F. Zhang, D. Wu, Y. Xu, and X. Feng, *J. Mater. Chem.*, 2011, **21**, 17590.
- (13) B. L. Rupert, W. L. Mitchell, A. J. Ferguson, M. E. Köse, W. L. Rance, G. Rumbles, D. S. Ginley, S. E. Shaheen and N. Kopidakis, *J. Mater. Chem.*, 2009, **19**, 5311.
- (14) G. Gigli, O. Inganäs, M. Anni, M. De Vittorio, R. Cingolani, G. Barbarella and L. Favaretto, *Appl. Phys. Lett.*, 2001, **78**, 1493.
- (15) M. Mazzeo, D. Pisignano, L. Favaretto, G. Barbarella, R. Cingolani and G. Gigli, *Synt. Met.*, 2003, **139**, 671.
- (16) M. Irie, T. Fukaminato, K. Matsuda and S. Kobatake, *Chem. Rev.*, 2014, **114**, 12174.
- (17) R. S. Becker, J. Seixas de Melo, A. L. Maçanita and F. Elisei, *J. Phys. Chem.*, 1996, **100**, 18683.
- (18) R. Weinkauff, L. Lehr, E. W. Schleg, S. Salzmann and C. M. Marian, *Phys. Chem. Chem. Phys.*, 2008, **10**, 393.

- (19) S. Salzmann, M. Kleinschmidt, J. Tatchen, R. Weinkauff and C. M. Marian, *Phys. Chem. Chem. Phys.*, 2008, **10**, 380.
- (20) G. Cui and W. Fang, *J. Phys. Chem. A*, 2011, **115**, 11544.
- (21) M. Stenrup, *Chem. Phys.*, 2012, **397**, 18.
- (22) D. Fazzi, M. Barbatti and W. Thiel, *Phys. Chem. Chem. Phys.*, 2015, **17**, 7787.
- (23) A. Prlj, B. F. E. Curchod, A. Fabrizio, L. Floryan and C. Corminboeuf, *J. Phys. Chem. Lett.*, 2015, **6**, 13.
- (24) C. Cocchi and C. Draxl, [arXiv:1502.07273](https://arxiv.org/abs/1502.07273)
- (25) J. Schirmer, *Phys. Rev. A*, 1982, **26**, 2395.
- (26) A. B. Trofimov and J. Schirmer, *J. Phys. B: At. Mol. Opt. Phys.*, 1995, **28**, 2299.
- (27) C. Hättig, *Adv. Quantum Chem.*, 2005, **50**, 37.
- (28) A. Dreuw and M. Wormit, *WIREs Comput. Mol. Sci.*, 2015, **5**, 82.
- (29) N. O. C. Winter, N. K. Graf, S. Leutwyler and C. Hättig, *Phys. Chem. Chem. Phys.*, 2013, **15**, 6623.
- (30) S. Knippenberg, D. R. Rehn, M. Wormit, J. H. Starcke, I. L. Rusakova, A. B. Trofimov and A. Dreuw, *J. Chem. Phys.*, 2012, **136**, 064107.
- (31) H. Li, R. Nieman, A. J. A. Aquino, H. Lischka and S. Tretiak, *J. Chem. Theory Comput.*, 2014, **10**, 3280.
- (32) H. Köppel, E. V. Gromov and A. B. Trofimov, *Chem. Phys.*, 2004, **304**, 35.
- (33) F. Plasser, R. Crespo-Otero, M. Pederzoli, J. Pittner, H. Lischka and M. Barbatti, *J. Chem. Theory Comput.*, 2014, **10**, 1395.
- (34) M. Barbatti, *J. Am. Chem. Soc.*, 2014, **136**, 10246.
- (35) M. Rubio, M. Merchán, E. Ortí and B. J. Roos, *J. Chem. Phys.*, 1995, **102**, 3580.
- (36) D. Beljonne, J. Cornil, R. H. Friend, R. A. J. Janssen and J. L. Brédas, *J. Am. Chem. Soc.*, 1996, **118**, 6453.
- (37) M. Rubio, M. Merchán, R. Pou-Amérgigo and E. Ortí, *ChemPhysChem*, 2003, **4**, 1308.
- (38) S. Seigert, F. Vogeler, C. M. Marian and R. Weinkauff, *Phys. Chem. Chem. Phys.*, 2011, **13**, 10350.

- (39) M. Andrzejak and H. A. Witek, *Theor. Chem. Acc.*, 2011, **129**, 161.
- (40) E. Stendardo, F. Avila Ferrer, F. Santoro and R. Improta, *J. Chem. Theory Comput.*, 2012, **8**, 4483.
- (41) F. Weigand and R. Alrichs, *Phys. Chem. Chem. Phys.*, 2005, **7**, 3297.
- (42) D. Rappoport and F. Furche, *J. Chem. Phys.*, 2010, **133**, 134105.
- (43) M. Barbatti, A. J. A. Aquino and H. Lischka, *Phys. Chem. Chem. Phys.*, 2010, **12**, 4959.
- (44) R. Crespo-Otero and M. Barbatti, *Theor. Chem. Acc.*, 2012, **131**, 1237.
- (45) M. Barbatti, M. Ruckebauer, F. Plasser, J. Pittner, G. Granucci, M. Persico and H. Lischka, *WIREs Comput. Mol. Sci.*, 2014, **4**, 26.
- (46) J. C. Tully, *J. Chem. Phys.*, 1990, **93**, 1061.
- (47) G. Granucci and M. Persico, *J. Chem. Phys.*, 2007, **126**, 134114.
- (48) F. Furche, R. Ahlrichs, C. Hättig, W. Klopper, M. Sierka and F. Weigend, *WIREs Comput. Mol. Sci.*, 2014, **4**, 91.
- (49) W. Humphrey, A. Dalke and K. Schulten, *J. Molec. Graph.*, 1996, **14**, 33.
- (50) C. Adamo and V. Barone, *J. Chem. Phys.*, 1999, **110**, 6158.
- (51) E. van Lenthe and E. J. Baerends, *J. Comput. Chem.*, 2003, **24**, 1142.
- (52) F. Wang and T. Ziegler, *J. Chem. Phys.*, 2005, **123**, 154102.
- (53) G. te Velde, F. M. Bickelhaupt, S. J. A. van Gisbergen, C. Fonseca Guerra, E. J. Baerends, J. G. Snijders and T. Ziegler, *J. Comput. Chem.*, 2001, **22**, 931.
- (54) C. Fonseca Guerra, J. G. Snijders, G. te Velde and E. J. Baerends, *Theor. Chem. Acc.*, 1998, **99**, 391.
- (55) ADF2013, SCM, Theoretical Chemistry, Vrije Universiteit, Amsterdam, The Netherlands, <http://scm.com>
- (56) E. Papajak, J. Zheng, H. R. Leverentz and D. G. Truhlar, *J. Chem. Theory Comput.*, 2011, **7**, 3027.
- (57) Frisch, M. J.; Trucks, G. W.; Schlegel, H. B.; Scuseria, G. E.; Robb, M. A.; Cheeseman, J. R.; Scalmani, G.; Barone, V.; Mennucci, B.; Petersson, G. A.; Nakatsuji, H.; Caricato, M.; Li, X.; Hratchian, H. P.; Izmaylov, A. F.; Bloino, J.; Zheng, G.; Sonnenberg, J. L.; Hada, M.; Ehara, M.; Toyota, K.; Fukuda, R.;

- Hasegawa, J.; Ishida, M.; Nakajima, T.; Honda, Y.; Kitao, O.; Nakai, H.; Vreven, T.; Montgomery, Jr., J. A.; Peralta, J. E.; Ogliaro, F.; Bearpark, M.; Heyd, J. J.; Brothers, E.; Kudin, K. N.; Staroverov, V. N.; Kobayashi, R.; Normand, J.; Raghavachari, K.; Rendell, A.; Burant, J. C.; Iyengar, S. S.; Tomasi, J.; Cossi, M.; Rega, N.; Millam, J. M.; Klene, M.; Knox, J. E.; Cross, J. B.; Bakken, V.; Adamo, C.; Jaramillo, J.; Gomperts, R.; Stratmann, R. E.; Yazyev, O.; Austin, A. J.; Cammi, R.; Pomelli, C.; Ochterski, J. W.; Martin, R. L.; Morokuma, K.; Zakrzewski, V. G.; Voth, G. A.; Salvador, P.; Dannenberg, J. J.; Dapprich, S.; Daniels, A. D.; Farkas, O.; Foresman, J. B.; Ortiz, J. V.; Cioslowski, J.; Fox, D. J.; Gaussian 09, Revision A.02, Gaussian, Inc., Wallingford CT, 2009.
- (58) L. González, D. Escudero and L. Serrano-Andrés, *ChemPhysChem*, 2012, **13**, 28.
- (59) D. M. P. Holland, A. B. Trofimov, E. A. Seddon, E. V. Gromov, T. Korona, N. de Oliveira, L. E. Archer, D. Joyeux and L. Nahon, *Phys. Chem. Chem. Phys.*, 2014, **16**, 21629.
- (60) E. J. Baerends, O. V. Gritsenko and R. van Meer, *Phys. Chem. Chem. Phys.*, 2013, **15**, 16408.
- (61) W. M. Flicker, O. A. Mosher and A. Kuppermann, *J. Chem. Phys.*, 1976, **64**, 1315.
- (62) R. Håkansson, B. Nordén and E. W. Thulstrup, *Chem. Phys. Lett.*, 1977, **50**, 305.
- (63) M. Dierksen and S. Grimme, *J. Phys. Chem. A*, 2004, **108**, 10225.
- (64) D. Jacquemin, A. Planchat, C. Adamo and B. Mennucci, *J. Chem. Theory Comput.*, 2012, **8**, 2359.
- (65) M. H. Palmer, I. C. Walker and M. F. Guest, *Chem. Phys.*, 1999, **241**, 275.
- (66) X. Wu, X. Zheng, H. Wang, Y. Zhao, X. Guan, D. L. Phillips, X. Chen and W. Fang, *J. Chem. Phys.*, 2010, **133**, 134507.
- (67) J. W. G. Bloom and S. E. Wheeler, *J. Chem. Theory. Comput.*, 2014, **10**, 3647.
- (68) D. E. Woon and T. H. Dunning Jr., *J. Chem. Phys.*, 1993, **98**, 1358.
- (69) B. F. E. Curchod, U. Rothlisberger and I. Tavernelli, *ChemPhysChem*, 2013, **14**, 1314.
- (70) J. C. Tully, *J. Chem. Phys.*, 2012, **137**, 22A301.

- (71) L. Serrano-Andrés, M. Merchán, M. Fülischer and B. O. Roos, *Chem. Phys. Lett.*, 1993, **211**, 125.
- (72) W. J. Buma, B. E. Kohler and T. A. Shaler, *J. Phys. Chem.*, 1994, **98**, 4990-4992.
- (73) D. V. Lap, D. Grebner and S. Rentsch, *J. Phys. Chem. A*, 1997, **101**, 107.
- (74) J. Seixas de Melo, L. M. Silva, L. G. Arnaut and R. S. Becker, *J. Chem. Phys.*, 1999, **111**, 12.
- (75) D. Beljonne, Z. Shuai, G. Pourtois and J. L. Bredas, *J. Phys. Chem. A*, 2001, **105**, 3899.
- (76) E. Fabiano, F. Della Sala, R. Cingolani, M. Weimer and A. Görling, *Chem. Phys. Lett.*, 2001, **339**, 343.
- (77) S. Samdal, E. J. Samuelsen and H. V. Volden, *Synth. Met.*, 1993, **59**, 259.
- (78) M. Kleinschmidt, J. Tatchen and C. M. Marian, *J. Comput. Chem.*, 2002, **23**, 824.
- (79) R. S. Becker, J. Seixas de Melo, A. L. Macanita and F. Elisei, *Pure&Appl. Chem.*, 1995, **67**, 9.
- (80) M. Persico and G. Granucci, *Theor. Chem. Acc.*, 2014, **133**, 1526.
- (81) M. Richter, P. Marquetand, J. González-Vázquez, I. Sola and L. González, *J. Chem. Theory Comput.*, 2011, **7**, 1253.
- (82) G. Cui and W. Thiel, *J. Chem. Phys.*, 2014, **141**, 124101.